COMMUNICATIONS

Magnetic Resonance in Medicine 50:659–663 (2003)

Sources of Plasma Glucose by Automated Bayesian Analysis of ^{2}H NMR Spectra

Matthew Merritt,[1*] G. Larry Bretthorst,[2] Shawn C. Burgess,[1] A. Dean Sherry,[1,3] and Craig R. Malloy[1,4]

Sources of blood glucose can be determined after oral ingestion of ^2H_2O followed by isolation of plasma glucose and measurement of the relative ^{2}H enrichments in select positions within the glucose molecule. Typically, ^{2}H enrichments are obtained by mass spectrometry but ^{2}H NMR offers an alternative. Here it is demonstrated that the entire analysis may be automated by Bayesian analysis of a ^{2}H free induction decay signal of monoacetone glucose to obtain a direct readout of the relative contributions of glycogenolysis, glycerol, and phosphoenol pyruvate to plasma glucose production. Furthermore, Markov Chain Monte Carlo (MCMC) simulations of the posterior probability density provide uncertainties in all metabolic parameters from a single patient, thereby allowing comparisons in glucose metabolism from one individual to another. The combined MCMC Bayesian methodology is operationally simple and requires little intervention from the operator. Magn Reson Med 50:659–663, 2003. © 2003 Wiley-Liss, Inc.

Key words: ^{2}H NMR; metabolism; gluconeogenesis; Bayesian analysis

Plasma glucose may originate from gastrointestinal absorption, glycogenolysis, or gluconeogenesis, and it has long been known that each contribution is highly sensitive to nutritional state. More recently, it has been shown that glucose metabolism may be abnormal among patients with common disorders, including cancer (1–3), cirrhosis (4,5), obesity (6), and diabetes (7,8). In general, however, glucose metabolism in humans is not widely studied because the methods to resolve sources of plasma glucose are time-consuming or impractical in typical clinical situations. Recently, the contributing sources to glucose production have been quantified by determining the relative enrichment of deuterium or tritium in specific carbon sites in glucose by mass spectrometry (9,10) after carbon-by-carbon chemical degradation of a glucose derivative. Despite the technical demands of this measurement, a diverse range of patients have now been examined, including low birthweight infants (11), children (12), lactating women (13), and others (14).

Deuterium (^{2}H) NMR may also be used to quantify ^{2}H enrichment in glucose (15,16). While ^{2}H NMR is attractive because all seven aliphatic deuterons in certain glucose derivatives can be resolved in a single experiment, the sensitivity is limited by the low levels of ^{2}H used in the human tracer experiments and the amount of glucose available in a few mL of blood. Given limited sensitivity, an operator-independent spectral analysis would be desirable. More importantly, it would also be desirable to establish a method which allowed a measure of the uncertainties in the metabolic parameters of interest from a single NMR measurement.

Numerous algorithms are available for fitting either the free induction decay or the Fourier-transformed spectrum to assure rapid, reproducible, and objective analyses. Bayesian probability theory is ideally suited to this analysis because of the abundance of prior knowledge available in a single ^{2}H NMR spectrum. Using this approach, the metabolic parameter estimates (posterior probability densities) can be based on both the prior information and data and the standard deviation of the resulting posterior probability densities directly indicate the uncertainty in the metabolic parameters of interest (18). In this study, oral ^2H_2O (9,10) was coupled with ^{2}H NMR, Bayesian inference, and Markov Chain Monte Carlo (MCMC) simulations to directly estimate the contributions of glycogenolysis, glycerol, and PEP to plasma glucose. This automated analysis of the ^{2}H FID is operator-independent and provides an estimate of error in each metabolic parameter from a single FID.

THEORETICAL BACKGROUND

Deuterium may be introduced into body water by oral administration of ^2H_2O. Plasma glucose then becomes enriched in ^{2}H at select metabolic steps in gluconeogenesis and glycogenolysis that involve exchange with cell water. The level of ^{2}H enrichment at H2, H5, and $H6_S$ depend on whether glucose originates with glycogen, glycerol, or PEP (Fig. 1) according to the following equations:

$$\text{glycogenolysis contribution} = 1\text{-}(H5/H2) \quad [1]$$

$$\text{glycerol contribution} = (H5 - H6(s))/H2 \quad [2]$$

$$\text{Krebs cycle contribution (PEP)} = H6(s)/H2. \quad [3]$$

[1]Department of Radiology, The Mary Nell and Ralph B. Rogers Magnetic Resonance Center, University of Texas Southwestern Medical Center, Dallas, Texas.

[2]Department of Chemistry and Radiology, Washington University, St. Louis, Missouri.

[3]Department of Chemistry, University of Texas at Dallas, Dallas, Texas.

[4]VA North Texas Health Care System, Dallas, Texas.

Grant sponsor: NIH-NCRR; Grant number: D2584.

Grant number: RR-02584; Grant sponsor: NCI; Grant number: R24-CA83060 (Washington University Small Animal Imaging Resource) (to G.L.B.).

*Correspondence to: Matthew Merritt, Ph.D., Mary Nell and Ralph B. Rogers Magnetic Resonance Center, Department of Radiology, University of Texas Southwestern Medical Center, 5801 Forest Park Road, Dallas, TX 75235-9085. E-mail: matthew.merritt@utsouthwestern.edu

Received 27 February 2003; revised 29 May 2003; accepted 30 May 2003.

DOI 10.1002/mrm.10577

Published online in Wiley InterScience (www.interscience.wiley.com).

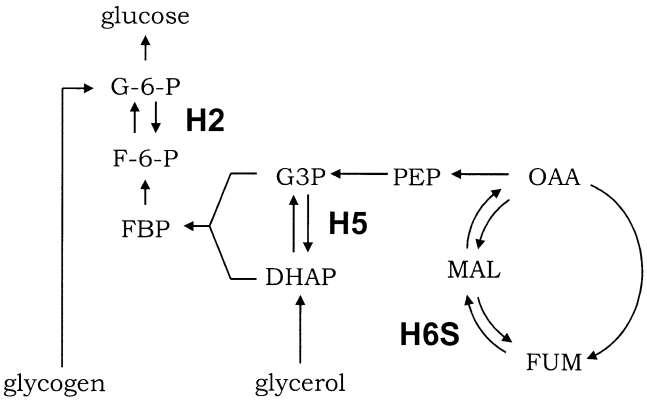

FIG. 1. Substitution of ^2H for ^1H in plasma glucose occurs due to different metabolic processes at each carbon. The labeling at H2 is equal to the level of enrichment in the body water. The areas of H5 and $H6_{(s)}$ vs. H2 measure the relative contributions of glycerol and PEP to gluconeogenesis.

Resonances associated with H1, H3, H4, and H6(r) are labeled by other metabolic pathways, but these signals are easily resolved from the pertinent resonances, and therefore do not interfere with the metabolic measurement. An initial bolus of ^2H_2O followed by maintenance doses is used to achieve a 0.3–0.5% body water enrichment. Plasma glucose is then converted to 1,2-O-isopropylidene-D-glucofuranose, hereafter referred to as monoacetone glucose (MAG) for analysis by either mass spectrometry (with further chemical processing) or directly by ^2H NMR.

Equations 1–3 may be solved given the ratios, H5/H2 and H6(s)/H2. Quantification of these independent ratios will be influenced by experimental variables such as signal-to-noise (S/N), linewidths, etc. Accurate fitting of H2, H5, and H6(s) require fitting of all 10 deuterium resonances in the spectrum (seven from MAG, one from HDO, and two from solvent acetonitrile). Bayesian theory provides a formal mechanism for evaluating the probability for each ratio, independent of all the parameters used in modeling the NMR signal. Further, the model is constrained by the prior knowledge from Eqs. [1]–[3] that $H2 \geq H5 \geq H6(s)$.

The Bayesian formulation relates Eqs. [1]–[3] directly to the spectrum and MCMC simulations (19) find a maximum for the probability density that takes into account the noise level for all three peaks simultaneously instead of a local maximum for each individual resonance. At high S/N levels the difference between conventional fitting and Bayesian/MCMC would be negligible, but with decreasing S/N the potential for erroneous metabolic results increases. The Bayesian/MCMC method quantifies this error in terms of an uncertainty in each metabolic parameter.

MATERIALS AND METHODS

The sample spectra illustrated in this article came from a single volunteer who participated in a larger study group. The protocol was reviewed and approved by the Institutional Review Board. The subject fasted overnight (14 hr) prior to the first dose of a 70/30 mixture of $^2H_2O/H_2O$. Three doses were given over the period of an hour with a total dose of 5 mg of ^2H_2O/kg body water where body water was assumed to be 60% of body weight. The fast continued for 42 hr, with maintenance doses of D_2O being given periodically. Blood (20 mL) was drawn at 14 and 42 hr, centrifuged at 2500 rpm to separate plasma extracted with perchloric acid, and converted to MAG (20). A ^2H NMR spectrum was collected at 14.1 T (92 MHz for ^2H) on a Varian INOVA console (Varian Instruments, Palo Alto, CA) with a 3 mm direct ^2H detect probe (Nalorac, Martinez, CA). ^1H Waltz-16 decoupling was used during acquisition to reduce linewidths in the ^2H spectrum. Data were collected over a spectral width of 1 kHz using single $\pi/2$ pulses with no delay between pulses. Given that the acquisition time was 1 sec and the longest T_1 of any deuteron in monoacetone glucose is less than 0.25 sec, no postacquisition correction of peak areas was necessary.

Bayesian Analysis and Markov Chain Monte Carlo Simulations

In order to infer the probabilities for the relative contributions of glycogenolysis, glycerol, and TCA cycle to blood glucose, it is necessary to relate the spectroscopic data to the metabolic model. The entire FID was modeled (18) and the sum rule of probability theory was used to reformulate the model in terms of ratios of resonance amplitudes necessary to solve Eqs. 1–3. In total, there are 39 different parameters in the model: an amplitude, frequency, and decay rate for each resonance (10 resonances in the spectrum, or 30 parameters) and an allowance for a bad first point, phase, and DC offsets in the real and imaginary channels for the FID and the metabolic model.

These 39 parameters are included in the expression for the joint posterior probability density. To estimate any single parameter, the other 38 dimensions must be integrated across to account for their influence on the probability of the chosen parameter (18). The only way to carry out integrals of such high dimensionality in a reasonable amount of time is through Monte Carlo integration (19). For this application we used 50 independent Markov chains (19) from which 50 independent samples were drawn from each chain for a total of 2500 different samples from the joint posterior probability density. After the samples were generated, sums were performed for each variable over the 2500 samples, producing estimates of the mean and standard deviation for each parameter.

To verify the accuracy of the analysis method, a variety of different datasets were simulated by summing a series of exponentially decaying sinusoids. For these datasets random noise with varying amplitude was added to the simulated free induction decays to decrease the S/N ratio and the simulated data was processed in the same manner as the data acquired from the spectrometer.

RESULTS AND DISCUSSION

Typical ^2H NMR spectra of monoacetone glucose derived from glucose present in 20 mL of whole blood are shown in Fig. 2a,c. The spectrum in Fig. 2a reflects plasma glucose after a 14-hr fast while the spectrum in Fig. 2c reflects glucose after a 42-hr fast. Simple visual inspection of the transformed spectra provides qualitative information

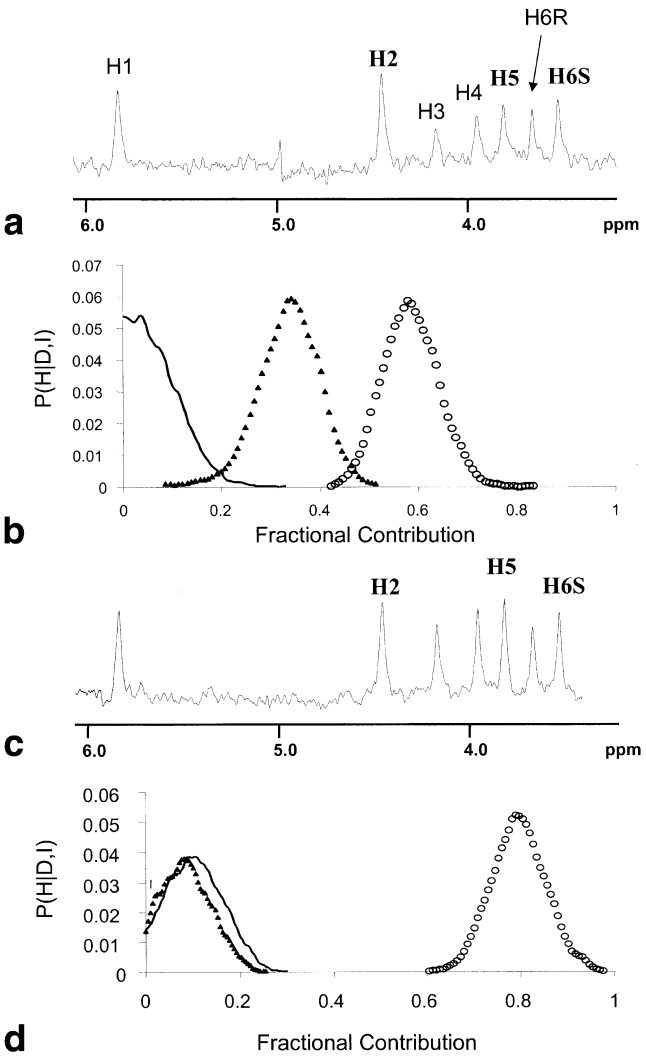

FIG. 2. Spectra and Bayesian/MCMC output for two NMR samples at 14 hr and 40 hr of fasting. Bold lettering indicates resonances used in calculation of metabolic values. The label for the y-axis is read, "The probability of the hypothesis given the data and the prior information." **a:** Spectrum for 14 hr of fast. **b:** The output of the program shows that the contribution from glycogen remains high (~34%). Glycogen is marked by triangles, TCA by open circles, and glycerol contribution by a solid line. **c:** Spectrum for 40 hr of fast. **d:** At 40 hr of fasting the contribution of glycogen has decreased while that of gluconeogenesis has increased significantly.

about the sources of plasma glucose at each time point. In Fig. 2a the H5/H2 ratio is low, indicating a significant contribution from glycogen. Also, the difference between $H6_S$ and H5 is small, indicating a very low contribution of glycerol to gluconeogenesis. At 42 hr (Fig. 2c), the H5/H2 ratio is ~1, showing that glycogen reserves were essentially depleted after this prolonged fast and H6S/H2 also approaches 1, indicating that most of the plasma glucose was generated from the level of the TCA cycle.

The results of the Bayesian/MCMC analysis of the free induction decays are shown as histograms in Fig. 2b,d. In contrast to focusing on the description of the spectrum (S/N, lineshape, etc.), the histograms immediately report the metabolic parameters plus give an estimate of the error in each metabolic parameter. For the 14-hr spectrum, the contributions to plasma glucose from glycogenolysis, gluconeogenesis from glycerol, and gluconeogenesis from PEP were 0.34 ± 0.06, 0.07 ± 0.05, and 0.58 ± 0.06, respectively. The sample collected at 42 hr reports contributions due to glycogenolysis, gluconeogenesis from glycerol, and gluconeogenesis from PEP were 0.09 ± 0.05, 0.11 ± 0.06, and 0.80 ± 0.06, respectively.

To assess the accuracy of the method, free induction decays composed of pregenerated sets of exponentially decaying sinusoids with four different levels of noise were analyzed. Figure 3 shows how one metabolic parameter, the TCA cycle contribution, is affected by increased noise in the spectrum. The vertical dotted line was obtained by performing the Bayesian analysis on data without noise. This of course reproduced the true TCA cycle contribution exactly; hence, the histogram has zero width. Increasing noise has two effects; it widens the histogram linearly (inset) and results, in the example shown, in a shift in the maximum of the probability density toward a slightly higher TCA cycle contribution. This is a systematic error caused by using the same set of noise with increasing amplitude. Here, the added noise either increased the intensity of $H6_S$ or decreased the intensity of H2 with a net result of a slight overestimate of the TCA cycle contribution from its true value. Although introduction of noise to a level similar to that typically seen experimentally (Fig. 2) did result in a slight overestimate of the TCA cycle contribution, the value determined was still within one standard deviation of the true value of this metabolic parameter.

A second way to assess the impact of noise upon metabolic estimates is to use the Bayesian model to fit an experimental FID, then use variations in the metabolic parameters to generate a new series of simulated free induction decays that have no noise and examine the residuals obtained by subtracting them from the data. Figure 4 shows the output of the MCMC analysis for the 42-hr sample. Using the metabolic parameters obtained from the maximum in each posterior probability density to synthesize a new spectrum results in a very small residual when

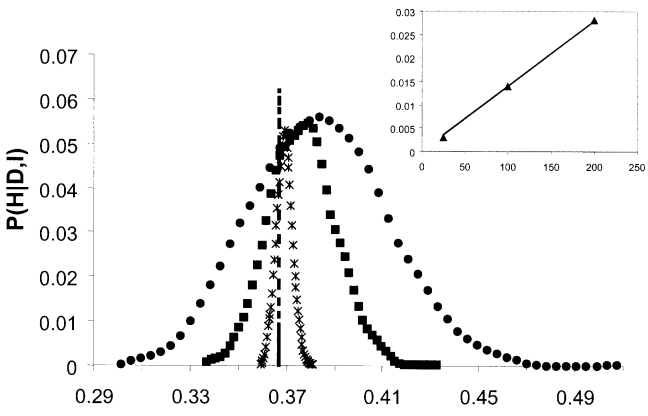

FIG. 3. Histograms for TCA cycle contribution as a function of decreasing S/N for the synthesized data. As the S/N decreases the histograms widen. The inset graphs the standard deviation of the estimate of the TCA contribution as a function of the applied noise power.

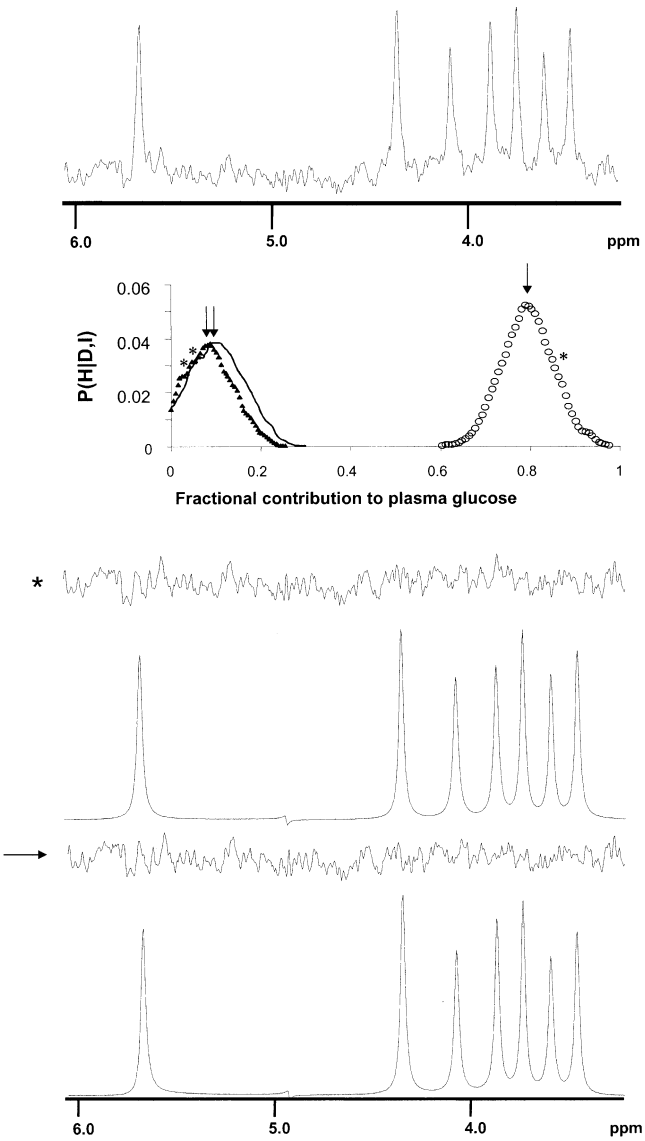

FIG. 4. Simulations and spectra for 40-hr fasting time point. The top spectrum displays the original NMR data. The second panel displays the histograms associated with the uncertainties in the metabolic parameters. Metabolic values that were not at the maximum of the probability densities denoted by the asterisks above the histograms were used to simulate the spectrum in the third panel. The bottom panel was obtained by simulating a spectrum using the values at the maximum of the probability densities, denoted by the arrows above the histograms. While the changes in the simulated spectra are subtle and the residuals show little difference to the eye, the metabolic values are significantly different from a physiological standpoint.

the two frequency domain spectra are subtracted (denoted in Fig. 4 by the arrows). This would be considered an excellent fit by any algorithm that uses frequency domain data. Interestingly, when a new set of metabolic parameters were chosen that fell closer to the tails of the probability distribution of the original Bayesian fit (the values denoted by the asterisk were 0.03, 0.06, and 0.91 for glycogenolysis, gluconeogenesis from glycerol, and gluconeogenesis from PEP, respectively), the residual seen in the frequency domain difference spectrum was not noticeably different to the eye from the fit drawn at the maximum of the probability distribution. This demonstrates that the time domain Bayesian analysis is more precise in evaluating these metabolic parameters than an operator-guided fit of frequency domain data. The set of values chosen at the tail of the probability distributions are nonphysiological (the values for glycogenolysis and glycerol contributions are too low, even for a 42-hr fast). Most importantly, it reveals that at this S/N level, an objective formulation of the error is essential. Spectra can be simulated which appear to account for the NMR data equally well, as evidenced by the residuals in Fig. 4, but do not correspond to the most probable estimate of the metabolic parameters. Our overall experience in fitting both time and frequency domain ^{2}H NMR spectra suggests that the Bayesian/MCMC analysis gives better estimates of metabolic parameters for spectra with S/N below 20. Above S/N ~20, both methods give similar results. Given that Bayesian analyses could be implemented to run without operator guidance in parallel with NMR data collection, this could become important for rapid throughput metabolic measurements.

If ^{2}H enrichment can be measured in the aliphatic hydrogens of plasma glucose, then it is a simple matter to calculate metabolic origins of glucose. The fact that each aliphatic deuteron can be detected directly by ^{2}H NMR in a single spectrum may prove to be an overwhelming advantage of NMR compared to mass spectrometry. Furthermore, NMR permits simultaneous examination of complex metabolic networks by tracers containing ^{13}C in addition to ^{2}H in a single experiment (15). Other methods for fitting the ^{2}H NMR data in either the time or frequency domain would locate the maximum of the probability density and hence produce a fit with an equally good residual, but the proposed method offers a systematic formulation of the uncertainty in the parameter estimates from a single spectrum. Since the prevalence of metabolic disorders such as obesity and type 2 diabetes is on the rise in our population, it is likely there will be increased demand for reliable and simple methods to evaluate glucose production in humans in the near future.

ACKNOWLEDGMENTS

Dr. Brian Weis processed the blood sample.

REFERENCES

1. Tayek JA, Katz J. Glucose production, recycling, Cori cycle, and gluconeogenesis in humans: relationship to serum cortisol. Am J Physiol 1997;272:E476–484.
2. Tayek JA, Manglik S, Abemayor E. Insulin secretion, glucose production, and insulin sensitivity in underweight and normal-weight volunteers, and in underweight and normal-weight cancer patients: a Clinical Research Center study. Metab Clin Exp 1997;46:140–145.
3. Richardson AP, Tayek JA. Type 2 diabetic patients may have a mild form of an injury response: a clinical research center study. Am J Physiol Endocrinol Metab 2002;282:E1286–1290.
4. Bugianesi E, Kalhan S, Burkett E, Marchesini G, McCullough A. Quantification of gluconeogenesis in cirrhosis: response to glucagon. Gastroenterology 1998;15:1530–1540.
5. Petersen KF, Krssak M, Navarro V, Chandramouli V, Hundal R, Schumann WC, Landau BR, Shulman GI. Contributions of net hepatic glycogenolysis and gluconeogenesis to glucose production in cirrhosis. Am J Physiol 1999;276:E529–535.

6. Gastaldelli A, Baldi S, Pettiti M, Toschi E, Camastra S, Natali A, Landau BR, Ferrannini E. Influence of obesity and type 2 diabetes on gluconeogenesis and glucose output in humans: a quantitative study. Diabetes 2000;49:367–1373.
7. Hundal RS, Krssak M, Dufour S, Laurent D, Lebon V, Chandramouli V, Inzucchi SE, Schumann WC, Petersen KF, Landau BR, Shulman GI. Mechanism by which metformin reduces glucose production in type 2 diabetes. Diabetes 2000;49:2063–2069.
8. Diraison F, Large V, Brunengraber H, Beylot M. Non-invasive tracing of liver intermediary metabolism in normal subjects and in moderately hyperglycaemic NIDDM subjects. Evidence against increased gluconeogenesis and hepatic fatty acid oxidation in NIDDM. Diabetologia 1998; 41:212–220.
9. Kuwajima M, Golden S, Katz J, Unger RH, Foster DW, McGarry JD. Active hepatic glycogen synthesis from gluconeogenic precursors despite high tissue levels of fructose 2,6-bisphosphate. J Biol Chem 1986; 261:2632–2637.
10. Landau BR, Wahren J, Chandramouli V, Schumann WC, Ekberg K, Kalhan SC. Use of 2H2O for estimating rates of gluconeogenesis, Application to the fasted state. J Clin Invest 1995;95:172–178.
11. Sunehag AL, Haymond MW, Schanler RJ, Reeds PJ, Bier DM. Gluconeogenesis in very low birth weight infants receiving total parenteral nutrition. Diabetes 1999;48:791–800.
12. Sunehag AL, Treuth MS, Toffolo G, Butte NF, Cobelli C, Bier DM, Haymond MW. Glucose production, gluconeogenesis, and insulin sensitivity in children and adolescents: an evaluation of their reproducibility. Pediatr Res 2001;50:15–123.
13. Sunehag AL, Louie K, Bier JL, Tigas S, Haymond MW. Hexoneogenesis in the human breast during lactation. J Clin Endocrinol Metab 2002; 87:297–301.
14. Roden M, Stingl H, Chandramouli V, Schumann WC, Hofer A, Landau BR, Nowotny P, Waldhausl W, Shulman GI. Effects of free fatty acid elevation on postabsorptive endogenous glucose production and gluconeogenesis in humans. Diabetes 2000;49:701–707.
15. Jones JG, Solomon MA, Cole SM, Sherry AD, Malloy CR. An integrated ^2H and ^{13}C NMR study of gluconeogenesis and TCA cycle flux in humans. Am J Physiol Endocrinol Metab 2001;281:E848–856.
16. Jones JG, Carvalho RA, Sherry AD, Malloy CR. Quantitation of gluconeogenesis by ^2H nuclear magnetic resonance analysis of plasma glucose following ingestion of ^2H_2O. Anal Biochem 2000;277:121–126.
17. Jaynes ET. Probability theory as logic. In: Fougere PF, editor, Maximum entropy and Bayesian methods. Dordrecht: Kluwer; 1990. p 1–16.
18. Bretthorst GL. An introduction to model selection using Bayesian probability theory. In: Heidbreder GR, editor. Maximum entropy and Bayesian methods. Dordrecht: Kluwer; 1996. p 1–42.
19. Gilks WR, Richardson S, Spiegelhalter DJ. Markov Chain Monte Carlo in practice. Boca Raton, FL: CRC Press; 1996.
20. Burgess SC, Weis B, Jones JG, Smith E, Merritt ME, Margolis D, Sherry AD, Malloy CR. Noninvasive evaluation of liver metabolism by 2H and 13C NMR isotopomer analysis of human urine. Anal Biochem 2003; 312:228–334.